Effects of Reaction Temperature on Microstructure and Advanced Pseudocapacitor Properties of NiO Prepared via Simple Precipitation Method

Qiangqiang Sun,   Shujuan Bao*

Abstract: Morphology-controlled synthesis and large-scale self-assembly of nanoscale building blocks into complex nanoarchitectures is still a great challenge in nanoscience. In this work, various porous NiO nanostructures are obtained by a simple ammonia precipitation method and we find that the reaction temperature has a significant impact on their microstructures. Nanoflowers and nanoflakes have been obtained at 0℃ and 50℃, while, weakly self-assembly nanoflowers with nanoflakes are formed at 20℃. In order to understand the process-structure-property relationship in nanomaterial synthesis and application, the as-prepared NiO is used as supercapacitor electrode materials, and evaluated by electrochemical measurement. The experimental results indicate that the material obtained at lower temperature has higher pseudocapacitance, the specific capacitance of 944, 889 and 410 F/g are reached for the materials prepared at 0℃, 20℃ and 50℃ and further calcined at 300℃, respectively. While the material obtained at higher temperature has excellent rate capacity. This offers us an opportunity searching for exciting new properties of NiO, and be useful for fabricating functional nanodevices.

Keywords: Nickel oxide; Temperature; Morphology; Pseudocapacitor

Introduction

In recent years, nanomaterials, with different dimensionalities and morphologies attract much attention due to their novel and unexpected properties. Generally, size, dimensionality and morphology of the materials have been regarded as critical factors that may bring some unique or improved properties. For example, mesoporous structured nanomaterials enable rapid diffusion across a large surface area, which result in reduced response time and enhanced interaction with the environment [1]. Hence, numerous studies have accordingly been carried out in an effort to exploit cost-effective method to synthesis nanostructured oxides with controllable shapes, composition, and pores in order to modify or promote their intrinsic properties. Nickel oxide is a kind of very attractive inorganic material due to its high capacity, natural abundance, low cost, and environmental friendliness. Morphology-controllable synthesis of NiO nanostructures has therefore a hot research topic for designing NiO nanomaterials with tunable properties.

Until now NiO with various morphologies, such as nanoparticles [2], nanoplates [3], nanotubes [4], nanowires [5], nanoribbons [6], hollow octahedral [7], nanowall [8], concave polyhedrons [9] and complex hierarchical nanostructures constructed with nanoscale building blocks [10] have been fabricated. And many different methods have been improved to synthesize the nanostructured NiO, such as chemical precipita-

Institute for Clean Energy & Advanced Materials, Southwest University, Chongqing 400715 China
*Corresponding author. E-mail: baoshj@swu.edu.cn

tion [11], sol-gel method [12], microemulsion technique [13], solvothermal methods [14,15], and so on. Among these synthetic approaches, the ammonia precipitation method is promising because of inexpensive raw material and simple processing. The researchers also found that the microstructure of NiO formed by ammonia precipitation can be tailored by reaction condition. For example, Deng [16] has prepared uniform nanocrystalline NiO particles which had cubic shapes with weak agglomerate. And Lang [17] has synthesized NiO with nano-flake structure. But there is no report on the influence of reaction temperature on the microstructure of products in precipitation reaction.

In this work, we have carefully investigated the influence of reaction temperature on the microstructure of products formed in ammonia precipitation and given a rational proposal about their forming mechanism. Importantly, it's first time to perform this reaction at 0℃. We dropped 5% aqueous ammonia to 1 M nickel nitrate in different temperature to form Ni(OH)$_2$. And after annealing at 300℃ for 3 h in air, we could get nickel oxides which have very different microstructure. The as-synthesized samples were characterized by X-ray diffraction (XRD), field emission scanning electron microscopy (FESEM), transmission electron microscopy (TEM) and nitrogen adsorption/desorption experiment for their microstructure and morphology. In order to investigate the effect of microstructure on performance, the as-prepared materials were used as electrochemical capacitor electrode materials, and some electrochemical techniques such as cyclic voltamogramm (CV) and electrochemical impedance spectroscopy (EIS) measurements were used to systematically study their microstructure-property relationship. The results indicate that the sample synthesized at 0℃ and further annealed at 300℃ although has a highest specific capacitance of 944 F/g at the current density of 1 A/g, its rate capacity is worse, which is closely related with its textural properties. It demonstrates that the reaction temperature has a big impact on the crystallinity, microstructure and performance of materials, which provide a new way for preparation advanced materials with high performance.

Experimental

Synthesis of NiO

Nickel nitrate hexahydrate was dissolved in deionized water (Ni concentration = 1.0 M) in a glass breaker under magnetic stirring. The nickel nitrate solution was slowly adjusted to pH=9 by dropping additional 5 wt% aqueous NH$_3$ for 2 h at the temperature of 0℃, 20℃ and 50℃, respectively. The resulting suspension was stirred at their temperature for another 2 h. Then the solid was filtered off, washed with a copious amount of

deionized water. After that, they were dried at 60℃ for 4 h in air, and then were annealed at 300℃ for 3 h.

Characterizationas and electrochemical tests

The crystal structure of the materials was characterized by powder XRD (XRD-7000). Morphology and microstructure of the synthesized materials were investigated by FESEM (S-4800, Japan) and TEM (JEM-2100). Nitrogen adsorption/desorption was carried out at 77.3 K by means of an ASAP 2020 X tended Pressure Sorption Analyzer. The surface area was calculated by using the Brunauer-Emmett-Teller (BET) equation. The pore size distribution (pore diameter, pore volume, and micropore surface area of the samples) was determined by the Barrett-Joyner-Halenda (BJH) method. And their hydrophilicity was evaluated by measuring contact angel (JC2000D1).

The electrodes of the electrochemical capacitors were fabricated by mixing the prepared powder with 15 wt% acetylene black and 5 wt% polytetrafluorene-ethylene binder of the total electrode mass. A small amount of alcohol was added to the mixture for a more homogeneous paste. The mixture was pressed onto nickel foam current collectors (1.0 × 1.0 cm^2) to make electrodes and the electrodes were dried at 80℃ for 16 h. Each electrode contains the active material in an area density of approximately 5.0 mg/cm^2. Electrochemical characterization was carried out in a conventional three-electrode cell in 6 M aqueous KOH electrolytes. Platinum foil and saturated calomel electrode (SCE) electrodes were used as the counter and reference electrodes, respectively. All electrochemical measurements were conducted using a CHI 660 electrochemical workstation (Shanghai Chenhua Co. Ltd., China).

Results and discussion

The XRD patterns of the Ni(OH)$_2$ precursor are shown in Fig. 1(A). It shows that the crystallinity of precursor increase with the reaction temperature going up. The pattern a and b corresponds to a layered α-Ni(OH)$_2$ structure with low crystallinity. For the precursor obtained at 50℃ (pattern c) displays three strong peaks, and all the diffraction peaks ascribe to well-crystallized β-phase hexagonal nickel hydroxide (JCPDS card, no.14-0117). The XRD patterns of samples formed by annealing the precursors at 300℃ for 3 h are shown in Fig. 1(B). And the diffraction peaks are in good agreement with the standard XRD pattern of the pure cubic phase of NiO (JCPDS card, no.73-1523) indicating that the pure phase of NiO is obtained by calcining Ni(OH)$_2$ precursor. Judging from the peaks intensity, after same sintering process, the sample which from the precursor obtained at 50℃ has

best crystallinity.

The surface morphology of the nanostructured NiO has been investigated using FESEM and TEM. It is clearly that the NiO obtained from different precursors exhibt different morphology (Fig. 2). The one which precursor obtained at 0℃ is very slack 3D flower-like microsphere in the SEM image, and the nanostructure of single flower-like microspheres consisting of many intercrossed thin nanoflakelets. While the sample which precursor formed at 20℃ is consist of some microspheres and some unequal-sized flakes. And the NiO which precursor obtained at 50℃ consists of uniform large flakes. The higher magnifications TEM further reveal the morphologies of the NiO whose precursors were formed at different temperature. And the results observed from TEM images are in agreement with that measured from SEM images.

The microstructure of the resultant NiO was further investigated by nitrogen adsorption-desorption experiments, as shown in Fig. 3. The nitrogen adsorption-desorption isotherms of the NiO obtained by different precursors all exhibited hysteresis loops of type IV curves, indicating the mesoporous characteristics of the obtained samples. According to BET analysis, the specific surface area of NiO sample whose precursor formed at 0℃, 20℃ and 50℃ is 135 m^2/g, 88 m^2/g and 42 m^2/g, respectively. What's more, the samples all have a mesopore size distribution. And the pores may come from the porous nanoflowers, the gap between particles or thick slices.
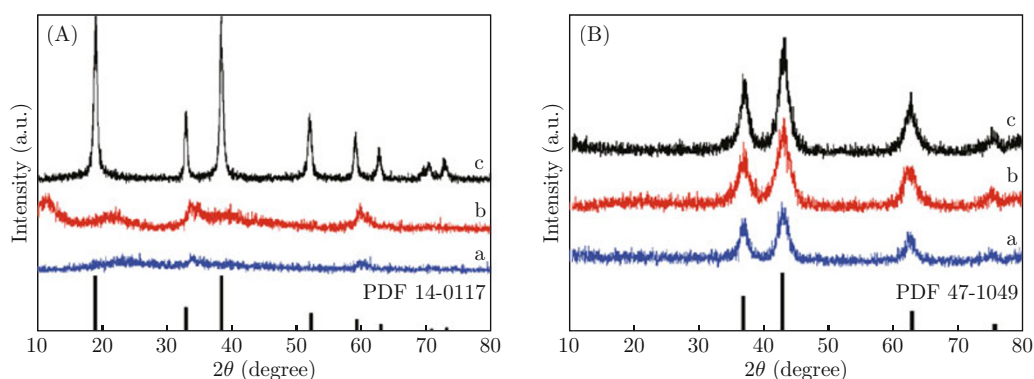

Fig. 1　The XRD patterns of (A) the Ni(OH)$_2$ precursor formed at (a) 0℃; (b) 20℃; (c) 50℃ and (B) the NiO obtained by annealed the precursors of (a) 0℃; (b) 20℃; (c) 50℃ at 300℃ for 3 h.
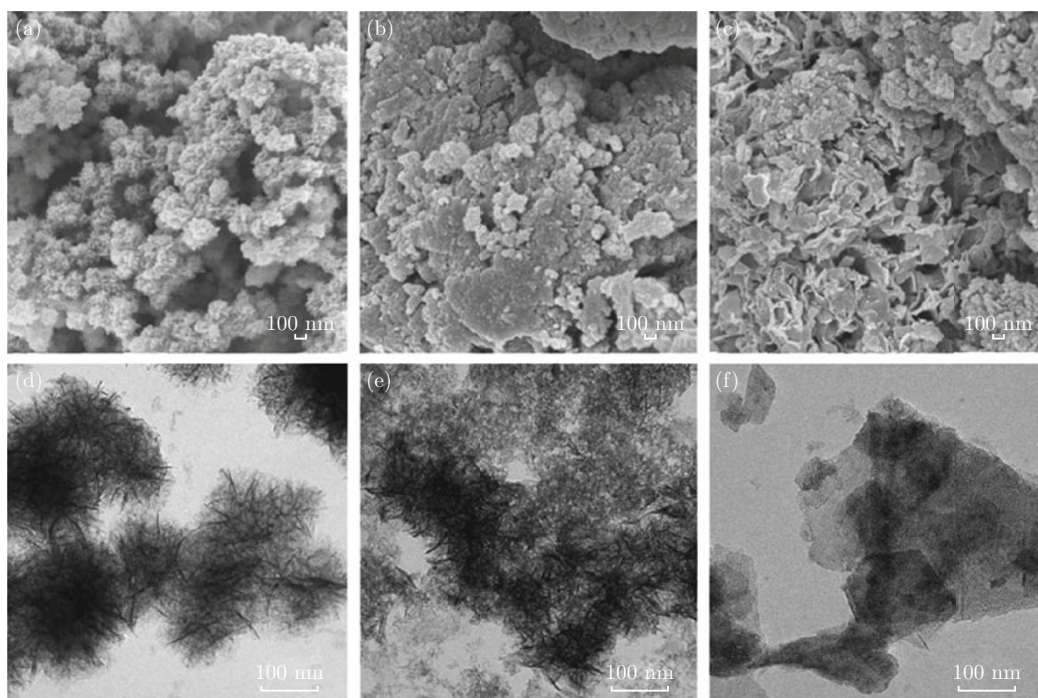

Fig. 2　SEM images (a, b, c) and TEM images (d, e, f) of NiO whose precursors were made at 0℃ (a, d), 20℃ (b, e) and 50℃ (c, f).
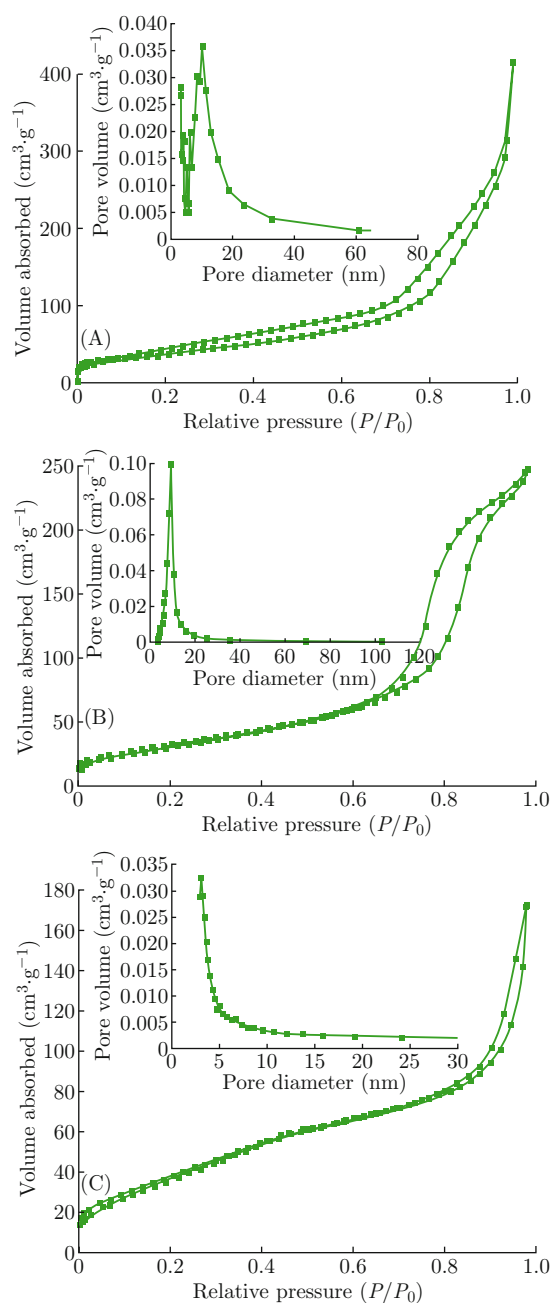
Fig. 3   BET isotherm of NiO whose precursors formed at (a) 0℃; (b) 20℃ and (c) 50℃. The inset is BJH pore size distribution.

The hydrophilicity of the samples fabricated in this work was further evaluated by water contact angle measurements. The water contact angles of the NiO which precusor from 0℃, 20℃ and 50℃ are 30.43°, 19.68°, 9.34°, respectively. Namely, after same sintering process, which precursor from higher temperature has excellent hydrophilicity. This result indicates that the reaction temperature has significant impact on the microstructures and crystallinity of the obtained materials, and further impacts their hydrophilicity.

It is very important to fully understanding the form-

ing mechanism of crystal growth in our reaction system for realizing the precise controlled synthesis of various defined nanostructure. On the basis of above experimental results, the possible growth process of different structures can be proposed and described as Fig. 4. In the reaction of forming $Ni(OH)_2$, Ni^{2+} ions in the solution are coordinated with $NH_3 \cdot H_2O$ to form $[Ni(NH_3)_x]^{2+}$ according to formula (1). The OH^- concentration is increased as the ammonia hydroxide solution is introduced into the solution, as shown in formula (2). Due to the increasing of OH^-concentration, the complex $[Ni(NH_3)_x]^{2+}$ are hydrolyzed into $[Ni(OH)_x]^{(x-2)-}$, as shown in formula (3). Then, $[Ni(OH)_x]^{(x-2)-}$ are dehydrated into $Ni(OH)_2$ precipitates.

$$Ni^{2+} + xNH_3 \cdot H_2O \rightleftharpoons [Ni(NH_3)_X]^{2+} + xH_2O \quad (1)$$

$$NH_3 \cdot H_2O \rightleftharpoons NH^{4+} + OH^- \quad (2)$$

$$[Ni(NH_3)_3]^{2+} + xOH^- \rightleftharpoons [Ni(OH)_X]^{(X-2)-} + xNH_3 \quad (3)$$
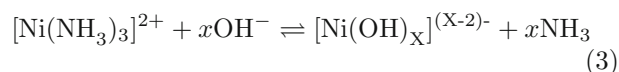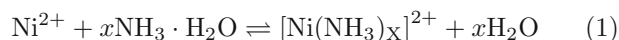
Figure 4 shows the schematic illustration of the major reactions involved in the synthesis process at different temperature. In the initial stage of the reaction, $[Ni(NH_3)_y]^{2+}$ are hydrolyzed to form $Ni(OH)_2$ nuclei. With the reaction going on, the primary $Ni(OH)_2$ nuclei change into $Ni(OH)_2$ nanoflakelets through a subsequent crystal growth process. At the same time, each nanoflakelets have their own orientated growth process. These grown progresses are related to both the anisotropic crystal structure of $Ni(OH)_2$ and the involved solution conditions. At 0℃, $Ni(OH)_2$ nanoflakelets grow very slowly, and from the thermodynamics point of view, the surface energy of the new formed nanoflakelets is quite high with two main exposed planes, and thus the neighboring nanosheets tended to grow togther form 3D $Ni(OH)_2$ flower-like microspheres by self-assembled [18]. As reported in literatures, the direct reason for self-assembly is crystal-face attraction, van der waals forces and hydrogen bonds [19,20]. For the reaction at 20℃, the reaction speed is faster than that of at 0℃, so it can produce much more primary particles, and much more nanoparticles are easy to form thicker nanaoflakelets with the crystal growth, due to its surface energy is lower the one got at 0℃, only part of the nanoflakelets self-assembled into nanoflowers. As for the situation at 50℃, the mechanism is similar to the first two, and the difference is that the nanofakelets are too thick to self-assemble into nanoflowers.

Remission of environmental and energy crises in recent years have wide applications especially in energy storage. It is well known that NiO has high pseudocapacity, and the NiO obtained in our work has very slack porous structure, which not only could boost ion and electron fast movement in electrochemical processes but
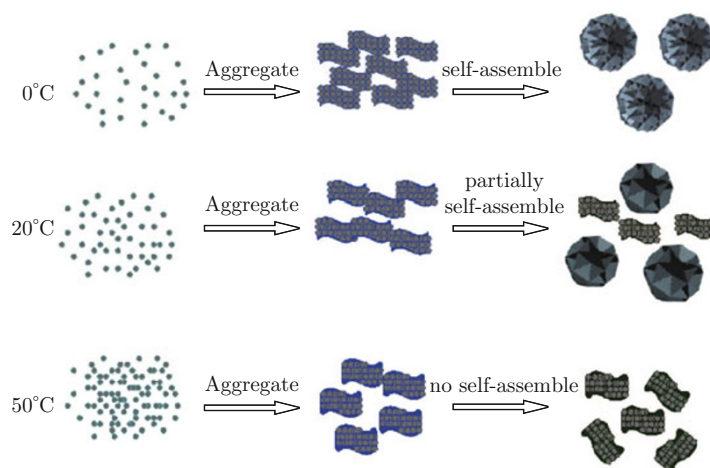
Fig. 4 Schematic illustration of the morphological evolution of the precursors formed at different temperature.
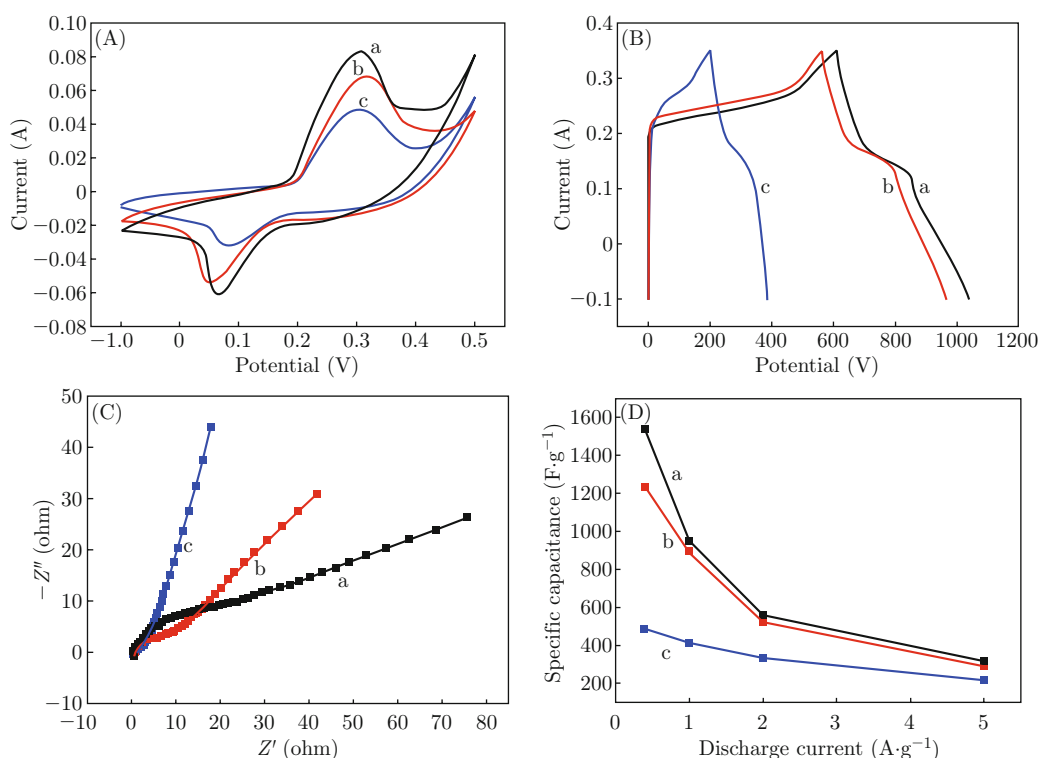

Fig. 5   (A) CV curves of NiO whose precursors was respectively synthesized at (a) 0℃; (b) 20℃; (c) 50℃ at the scanning rate of 5 mV/s. (B) Galvanostatic charge and discharge curves of NiO with a current density of 1 A/g. (C) Nyquist plots for NiO electrode at potential of 0.1 V. (D) the capacitances under different discharge current.

also have big specific surface area. Hence, the as-synthesized materials were used as electrochemical capacitor electrode materials to estimate the process-structure-property relationship of the obtained NiO in this work.

As shown in Fig. 5(A), all the as prepared NiO whose precursor obtained at different temperature show a pair of redox peaks in the CV curves, which due to the following reversible electrochemical reaction.

$$NiO + OH^- \rightleftharpoons NiOOH + e^- \qquad (4)$$

Among of these CV curves, the area under the CV curve for NiO whose precursor obtained at 0℃ is apparently larger than that of other samples, and the order of their area is a > b > c, demonstrating that the NiO whose precursor formed at lower temperature has higher capacitance, possibly due to its more slack structure and larger specific surface area.

The charge-discharge performance measurements were further used to estimate the pseudocapacity properties of as-prepared materials. As shown in Fig. 5(B), during the charge and discharge steps, the curves dis-

play two variation ranges. A perfect variation of potential vs. time (below about 0.1 V) parallel to the potential axis indicates a pure double-layer capacitance behavior from the charge separation at the electrode/electrolyte interface, and a sloped variation of the potential vs. time (0.1∼0.35 V) shows a typical pseudocapacitance behavior, caused by the electrochemical adsorption/adsorption or redox reaction at the electrode/electrolyte interface. The specific capacitance of the electrodes at a current density of 1 A/g is calculated by $C = \frac{I \times \Delta t}{\Delta V \times m}$ from the discharge curves, where I is the constant discharge current, Δt is the discharge time, ΔV is the potential drop during discharge, and m is the mass of NiO. The specific capacitance value is 944, 889 and 410 F/g were calculated for the materials prepared at 0℃, 20℃ and 50℃ and further calcined at 300℃, respectively.
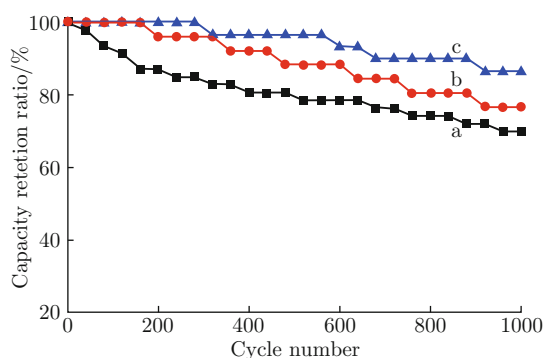

Fig. 6 Cycle life of as-prepared NiO electrode at a discharge current of 1 A/g and a, b, c stands for the sample whose precursor synthesized at 0℃, 20℃ and 50℃, respectively.

To further investigate the influence of such nanostructure on electrolyte diffusion, EIS was conducted on the prepared NiO. Figure 5(C) shows the Nyquist plots of the prepared NiO at the potential of 0.1 V with a frequency range from 10^5 to 0.01 Hz in 6 M KOH. The Nyquist plots (Fig. 5(C)) show well-defined semicircles over the high frequency range, followed by straight sloped line in the low-frequency region for both samples. The diameter of the semicircle corresponds to the interfacial charge-transfer resistance (R_{ct}), which usually represents the resistance of electrochemical reactions on the electrode and is called the Faraday resistance, and the straight line is ascribed to the diffusive resistance (Warburg impendence, W) of electrolyte in electrode pores and the proton diffusion in host materials. As shown in Fig. 5(C), the nanoflake-shaped NiO exhibits a smaller semicircle than the other two at the high-frequency region, implies that the nanoflake has the lowest charge-transfer resistance, which may due to its higher crystallinity, and good hydrophilicity. However, the nanoflower-shaped NiO has a lowest slope, implying that the ion diffusion or

transport is the most difficult in it. This can be explained by their hydrophilicity, the specimen formed at 50℃ has a worse hydrophilicity than that of formed at 0℃ and 20℃. And the hydrophilicity of electrode materials will affect the diffusion of electrolyte in electrode materials. Furthermore, as shown in Fig. 5(D), the flower-liked NiO sphere has a worst rata capacity, while the NiO nanofakelets have best rate capacity.

Since long cycle life is very important to the supercapacitor, the charge/discharge cycles test was employed to examine the service life of the obtained different NiO. Figure 6 shows the capacitance loss of the different NiO based electrodes with 1000 cycles. With the increasing of cycle number, the discharge capacitance for all the different NiO based electrodes is decrease gradually, and after 1000 cycles, for the NiO whose precursors was synthesized at 50℃ retain 90% of its initial capacity, while the capacity-keeping rate of the NiO whose precursors was synthesized at 0℃ is only 70%. This indicated that the NiO has a high degree of crystallinity, suitable pore size distribution and little bigger particles size is more stable during the long charge and discharge processes.

Conclusion

A simple and effective ammonia precipitation method has been put forward to build different microstructured NiO by just adjusting the reaction temperature. It is found that the precipitation temperature has a great influence on the microstructure, hydrophilicity and electrochemical performance of products. Nanoflower liked NiO sphere could obtain at 0℃, while, NiO nanoflakes are formed at 20℃. The electrochemical results indicated that the nanoflower liked NiO has a highest specific capacity of 1538 F/g at a current density of 0.4 A/g, which is closed to the highest capacity of 1609 F/g reported by literatures so far [20], but its capacity obviously decreased with the increasing of current density. What's more, although the specific capacity of NiO nanoflakes is not very high, its rate capacity is excellent. All of these suggested that the preparation approach and microstructure of materials has a significantly impact on their electrochemical performance. Hence, to realize the full controlled synthesis of nanomaterials is very important for their applications. According to our experimental results, not only large surface area and porous structure but good hydrophilicity has a significantly impact on the electrochemical performance of NiO. Hence, further improvement of this experiment should be focused on enhancing the hydrophilicity of NiO whose precursor formed at 0℃, introduce surfactant into the reaction solution may be a good choice [21] .

Acknowledgements

References

[1] B. J. Melde and B. J. Johnson, "Mesoporous materials in sensing: morphology and functionality at the meso-interface", Anal. Bioanal. Chem. 398(4), 1565-73 (2010). http://dx.doi.org/10.1007/s00216-010-3688-6

[2] Q. Li, L.-S. Wang, B.-Y. Hu, C. Yang, L. Zhou and L. Zhang, "Preparation and characterization of NiO nanoparticles through calcination of malate gel", Mater. Lett. 61(8-9), 1615-1618 (2007). http://dx.doi.org/10.1016/j.matlet.2006.07.113

[3] Z.-H. Liang, Y.-J. Zhu and X.-L. Hu, "β-Nickel hydroxide nanosheets and their thermal decomposition to nickel oxide nanosheets", J. Phys. Chem. Lett. B 108(11), 3488-3491 (2004). http://dx.doi.org/10.1021/jp037513n

[4] S. A. Needham, G. X. Wang and H. K. Liu, "Synthesis of NiO nanotubes for use as negative electrodes in lithium ion batteries", J. Power Sources 159(1), 254-257 (2006). http://dx.doi.org/10.1016/j.jpowsour.2006.04.025

[5] C. Xu, K. Hong, S. Liu, G. Wang and X. Zhao, "A novel wet chemical route to NiO nanowires", J. Cryst. Growth 255(3-4), 308-312 (2003). http://dx.doi.org/10.1016/s0022-0248(03)01246-6

[6] K. Matsui, B. K. Pradhan, T. Kyotani and A. Tomita, "Formation of nickel oxide nanoribbons in the cavity of carbon nanotubes", J. Phys. Chem. Lett. B 105(24), 5682-5688 (2001). http://dx.doi.org/10.1021/jp010496m

[7] X. Wang, L. Yu, P. Hu and F. Yuan, "Synthesis of single-crystalline hollow octahedral NiO", Crystal Growth & Design 7(12), 2415-2418 (2007). http://dx.doi.org/10.1021/cg060957z

[8] B. Varghese, M. Reddy, Z. Yanwu, C. S. Lit, T. C. Hoong, G. Subba Rao, B. Chowdari, A. T. S. Wee, C. T. Lim and C.-H. Sow, "Fabrication of NiO nanowall electrodes for high performance lithium ion battery", Chem. Mater. 20(10), 3360-3367 (2008). http://dx.doi.org/10.1021/cm703512k

[9] W. Zhou, M. Yao, L. Guo, Y. Li, J. Li and S. Yang, "Hydrazine-linked convergent self-assembly of sophisticated concave polyhedrons of beta-Ni (OH)$_2$ and NiO from nanoplate building blocks", J. Am. Chem. Soc. 131(8), 2959-2964 (2009). http://dx.doi.org/10.1021/ja808784s

[10] J. Liu, S. Du, L. Wei, H. Liu, Y. Tian and Y. Chen, "Template-free synthesis of NiO hollow microspheres covered with nanoflakes", Mater. Lett. 60(29), 3601-3604 (2006). http://dx.doi.org/10.1016/j.matlet.2006.03.068

[11] M.-S. Wu and H.-H. Hsieh, "Nickel oxide/hydroxide nanoplatelets synthesized by chemical precipitation for electrochemical capacitors", Electrochimica Acta 53(8), 3427-3435 (2008). http://dx.doi.org/10.1016/j.electacta.2007.12.005

[12] Q. Yang, J. Sha, X. Ma and D. Yang, "Synthesis of NiO nanowires by a sol-gel process", Mater. Lett. 59(14-15), 1967-1970 (2005). http://dx.doi.org/10.1016/j.matlet.2005.02.037

[13] P. Palanisamy and A. M. Raichur, "Synthesis of spherical NiO nanoparticles through a novel biosurfactant mediated emulsion technique", Mater. Sci. Eng. C 29(1), 199-204 (2009). http://dx.doi.org/10.1016/j.msec.2008.06.008

[14] E. R. Beach, K. Shqau, S. E. Brown, S. J. Rozeveld and P. A. Morris, "Solvothermal synthesis of crystalline nickel oxide nanoparticles", Mater. Chem. & Phys. 115(1), 371-377 (2009). http://dx.doi.org/10.1016/j.matchemphys.2008.12.018

[15] Hua Jiao, "Urchin-like NiO Superstructures Prepared by Simple Thermal Decomposition Process", Nano-Micro Lett. 3(3), 166-170 (2011). http://dx.doi.org/10.3786/nml.v3i3.p166-170

[16] J. W. Lang, L. B. Kong, W. J. Wu, Y. C. Luo and L. Kang, "Facile approach to prepare loose-packed NiO nano-flakes materials for supercapacitors", Chem. Commun. 35, 4213-4215 (2008). http://dx.doi.org/10.1039/B800264A

[17] J. Huang, Y. Wu, C. Gu, M. Zhai, K. Yu, M. Yang and J. Liu, "Large-scale synthesis of flowerlike ZnO nanostructure by a simple chemical solution route and its gas-sensing property", Sens. Act. B: Chem. 146(1), 206-212 (2010). http://dx.doi.org/10.1016/j.snb.2010.02.052

[18] L. S. Zhong, J. S. Hu, H. P. Liang, A. M. Cao, W. G. Song and L. J. Wan, "Self-Assembled 3D flowerlike iron oxide nanostructures and their application in water treatment", Adv. Mater. 18(18), 2426-2431 (2006). http://dx.doi.org/10.1002/adma.200600504

[19] S. Zeng, K. Tang, T. Li, Z. Liang, D. Wang, Y. Wang, Y. Qi and W. Zhou, "Facile route for the fabrication of porous hematite nanoflowers: its synthesis, growth mechanism, application in the lithium ion battery, and magnetic and photocatalytic properties", J. Phys. Chem. Lett. C 112(13), 4836-4843 (2008). http://dx.doi.org/10.1021/jp0768773

[20] H. Pang, B. Zhang, J. Du, J. Chen, J. Zhang and S. Li, "Porous nickel oxide nanospindles with huge specific capacitance and long-life cycle", RSC Adv. 2 (6), 2257-2261 (2012).

[21] B. Chang, X. Zhang, J. Guo, Y. Sun, H. Tang, Q. Ren and W. Yang, "General one-pot strategy to prepare multifunctional nanocomposites with hydrophilic colloidal nanoparticles core/mesoporous silica shell structure", Journal of colloid and interface science. 377 (1), 64-75 (2012).